

Dynamic studies of proton diffusion in mesoscopic heterogeneous matrix

I. Concentrated solutions of sucrose

M. Gutman, E. Nachliel, and S. Kiryati

Laser Laboratory for Fast Reactions in Biology, Department of Biochemistry, The George S. Wise Faculty of Life Sciences, Tel Aviv University, Ramat Aviv 69978 Israel

ABSTRACT Biochemical systems lose their homogeneity at a mesoscopic scale; physical parameters vary sharply over a scale of a few nanometers.

In this manuscript, we demonstrate how proton diffusion studies can report the microscopic properties of inhomogeneous systems.

The method used for this purpose was the laser induced proton pulse and the reaction followed was the recombination of a proton with pyranine anion (8 hydroxy pyrene 1,3,6 trisulfonate) either in the excited state (subnanosecond dynamics) or in the ground state (microsecond time-scale measurements). The observed signals were analyzed by numeric integration of differential rate equations pertinent to the diffusion controlled reaction between proton and pyranine anion.

The accuracy of the methodology was verified by measuring the dielectric constant of sucrose solutions. The results we obtained are identical with those published in the International Critical Tables (1933. Vol. VI, 82-101).

The diffusion coefficient of proton was found to be independent of the sucrose concentration, up to 2M solution where the sucrose makes up 45% of the volume. This observation is interpreted in terms of the microscopic heterogeneity of the solution: the proton diffuses in the aqueous space between the sucrose molecules, while the continuity of the aqueous phase is maintained by the Brownian motion of the sucrose molecule, which allows the proton to pass between them at an unhindered rate.

INTRODUCTION

The space confined between lipid membranes or proteinaceous structures, the environment where biochemical reactions take place, is mesoscopic in size. It is large enough for ions or solutes to exist in their fully hydrated state, yet sufficiently small to bear the mark of a constant influence of the adjacent, low dielectric, matrix of the membrane or the protein.

The presence of these structural elements affects the properties of ions in two ways: (a) The dielectric boundary intensifies the electrostatic interactions (Matthew and Richards, 1982; Kjellander and Marcelja, 1988; Mathias et al., 1991), leading to an expansion of the Coulomb cage, where the electrostatic potential is larger than thermal energy. (b) The nonpermeability of the boundary structures reduce the dimensionality of the reaction space, leading to first passage time which is shorter than in spheric symmetric space (Adam and Delbruck, 1968; Berg and Purcell, 1977; Hardt, 1979).

To measure the reactivity of ions at the surface of membrane or protein, one must isolate the events proceeding within this space of interest from the huge bulk volume in which the structures under study are suspended. What is more, to focus on the limited space, the observation period must be sufficiently short to prevent exchange of ions between the small space being studied and the suspending solution.

In the present publication we wish to demonstrate how the dynamics of proton transfer can be used as a probing reaction for a mesoscopic space and what information can be gained.

The studies are focussed on a simple model system in which the proton impermeable matter is in a molecular

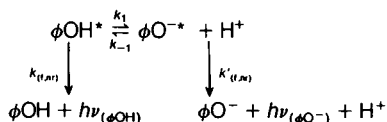
homogeneous dispersion, thus, one can adhere to a continuum symmetric model of the reaction space. In the following publication, we shall address a more organized system where the aqueous phase is confined between phospholipid membranes.

The space studied in this publication is the aqueous phase in sucrose solution. Sucrose dissolved in water behaves as an almost ideal solution (Robinson and Stokes, 1959) and the activity coefficient of water is close to unity even when 45% of the solution's volume is taken by the dissolved sugar. At such high concentrations of solute, the water molecules do not form a continuous body. They are "squeezed" between the dissolved sucrose molecules, forming microscopic spaces of bulk water separated from each other by sucrose molecules. Still, due to the relative motion of the solute, the spatio-temporal connectivity of the aqueous matrix is maintained.

Propagation of a particle in this heterogeneous medium will consist of two mechanisms: a normal diffusion process in the microscopic aqueous space, and a passage from one aqueous "pocket" to another during the Brownian motion of the sucrose molecules. The effect of the heterogeneity will vary with the observation time. If the observation of ion propagation is as short as its passage time within a continuous aqueous body, there will be no evidence for the presence of the nonpenetrable boundaries made by the dissolved sugar. A longer observation period will also reflect the obstruction of path effect (Robinson and Stokes, 1959). Thus, the nature of the results may vary with the length of the observation time.

We measured the propagation of proton in the water-sucrose system in three time intervals. For the microsec-

Address correspondence to Dr. Gutman.



SCHEME I

ond and subnanosecond measurements we used the laser induced proton pulse (Gutman, 1986; Gutman and Nachliel, 1990). The observation is based on photoexcitation of pyranine (8 hydroxy pyrene 1,3,6 trisulfonate), a compound which upon excitation becomes strong acid and ejects its hydroxyl proton (see Scheme I). In the microsecond time window, we follow the reprotonation of ΦO^- generated by the relaxation of the excited anion ΦO^{*-} . Its reprotonation follows a homogeneous second-order bimolecular kinetics. The subnanosecond dynamics rely on time resolved fluorescence where the just dissociated proton reacts by a geminate recombination process with its sibling ΦO^{*-} . The analysis of the dynamics produces the chemical properties of the reacting molecule and the physical properties of the matrix through which the proton diffuses.

The longest observation method is conductivity measurements where the field polarity is reversed at 70 Hz.

From these three modes of measurements we deduce parameters like the dielectric constant of the solution, the diffusion coefficient of the proton and the exposure of the pyranine to free water. The privilege of measuring the same reaction over a time range of six orders of magnitude allows us to interpret the observation in a concise and comprehensive way.

MATERIALS AND METHODS

Pyranine (8 hydroxy pyrene 1,3,6 trisulfonate) laser grade was supplied by Eastman Kodak Co. (Rochester, NY). Sucrose, enzyme grade, was by Sigma Chemical Co. (St. Louis, MO). All solutions were made in bidistilled water.

Time resolved fluorescence dynamics were carried out with a picosecond laser system consisting of a mode locked Yag laser, cavity damping dye laser and second harmonic generator delivering 1ps (full width at half maximum) pulse ($\lambda = 300$ nm) at a frequency of 700 KHz. The fluorescence was monitored by a time correlated single photon counting system. The time resolution of the whole system is 50 ps. For more details see Huppert et al. (1990).

Time resolved transient absorption measurements: the incremental absorption of the pyranine anion (ground state) following photodissociation of the proton was measured with a system consisting of a Q switched Yag laser and CW argon laser. The excitation was carried out with the third harmonic frequency of the Yag and incremental absorption was followed with the 457-nm band of the argon laser. The time resolution of the whole system was 20 ns. For details see Gutman (1986).

Conductivity measurements were carried out at 25°C using Radiometer CDM 2d conductivity meter operating at 70 Hz.

Analytical treatment

The model used for the analysis of the time resolved fluorescence of ΦOH^* is given in Scheme II.

The proton is originated from the pyranine molecule represented by a reaction sphere (R_0). This sphere is centered around the pyranine's hydroxyl and represents the minimal distance where a free hydrated proton can exist. Whenever a proton enters into the reaction sphere, a step characterized by k_r (given in cm/s units, (Pines et al., 1988), the formation of ΦOH^* is too fast to be resolved at our picosecond resolution. Similarly, when the proton dissociates from ΦOH^* (given by k_f , in s^{-1} units), we cannot detect the events before it appears at R_0 . At present time resolution we regard R_0 as the contact distance between the fully hydrated proton and ΦO^{*-} species. In dilute aqueous solution, the proton can be ejected in all directions. At high concentrations of sucrose, where contact between dye and sucrose molecules takes place, the situation is different. The proton can be ejected only to the aqueous phase where it is rapidly hydrated. Thus, that fraction of the reaction sphere's surface, which is taken by sucrose molecule, is blocked for protolytic reactions. This partial masking of the surface of the reaction sphere is treated as a steric factor σ , which will be discussed later.

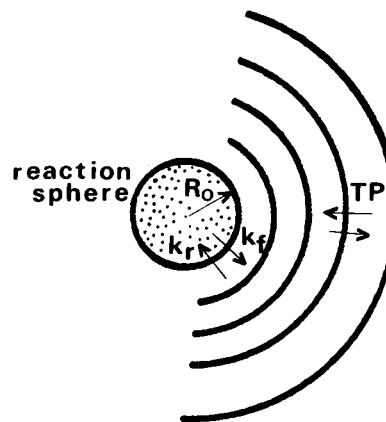
The diffusion of the proton is described as consecutive transition between concentric spheric shells with a width of Δr . The probability of transition between two adjacent shells, r_i and r_j , is given by the equation derived by Agmon (Agmon and Szabo, 1990; Pines et al., 1988; Huppert et al., 1990).

$$TP_{i/j} = \frac{D_{H^+}}{\Delta r^2} \cdot \frac{r_i}{r_j} \cdot \exp\left[-\frac{R_D}{2} \left(\frac{1}{r_i} - \frac{1}{r_j}\right)\right]. \quad (1)$$

There are three terms in Eq. 1 and all of them describe the properties of the diffusion matrix. The first one includes the diffusion coefficient of the proton. The second term, the ratio between the shell's radii, is a geometric term indicating the gradient of the incremental volume of the shells. The last term is the gradient of the electrostatic potential, where R_D is the distance where the dielectrics of the medium reduce the electrostatic ion pair potential to the value of the thermal energy.

$$R_D = |Z_1 \cdot Z_2| e_0^2 / \epsilon kT.$$

Thus, the exponential term in Eq. 1 represents the dielectric constant of the diffusion space.



SCHEME II Definition of the parameters needed for the numeric reconstruction of the fluorescence decay dynamics modulated by geminate recombination.

The excited molecule (ΦOH^*) is defined by a reaction sphere (R_0). On its perimeter, the proton is produced by dissociation (given by rate constant k_f) or consumed (at a rate constant, k_r). The proton diffuses between the concentric shells at a rate given by the diffusion coefficient (D_{H^+}) while the transition probability (TP) of stepping inward or outward is controlled by the gradient of the electrochemical potential field (see Eq. 1).

Agmon's computer program propagates the proton within the matrix of the transition probabilities using numerical methods. By varying the adjustable parameters of the program, the observed fluorescence decay can be reconstructed with a high level of accuracy. For details see Pines et al. (1988); Huppert et al. (1990); and Agmon and Szabo (1990).

Proton-pyranine anion reaction, in the microsecond time scale, were analyzed by numerical solution of nonlinear differential rate equation using the DVERK program of IMSL (For details see Gutman, 1984, 1986).

RESULTS

Geminate recombination in concentrated sucrose solution

In its excited state (ΦOH^*), pyranine is a strong acid. The hydroxyl proton dissociates with a time constant of ~ 100 ps (Pines et al., 1988). The conjugate acid, ΦO^{*-} , with its strong electrostatic field ($Z = -4$) may recapture the proton just ejected even before it equilibrates with the population of protons present in the solution. This reaction, called geminate recombination, has a clear mark of identity: the relaxation of the ΦOH^* emission exhibits a nonexponential decay dynamics (Huppert et al., 1990), easily detected as a long persistent "tail" of fluorescence dynamic curve (see Fig. 1, *A* and *D*). In low concentrations of sucrose (i.e., ~ 50 mM), the dynamics are exactly as measured in pure water (not shown). As the concentration of sucrose increases, the initial decay of ΦOH^* emission is slowed while the magnitude of the tail increases.

The reconstruction of the observed signal by Agmon's numerical solution is attained by assigning discrete values to the following parameters to obtain a theoretical curve which is identical to the experimental results. Three of the parameters, k_f , k_r , and R_0 , describe the properties of the excited dye molecule and its hydration shell. The other two, D_{H^+} and ϵ (or R_D) characterize the properties of the diffusion space.

Each of the parameters controls mostly, one feature of the dynamics: k_f , the rate of proton dissociation, determines the decay within the first 100 ps or so. The curvature of the transition from the rapid decay into the long tail, better seen in the logarithmic plots (Fig. 1, *D*, *E*, and *F*) is controlled by ϵ while the final shape of the decay is controlled by D_{H^+} with secondary contribution of R_0 and k_r .

In our simulation we analyzed the dynamics starting with dilute solutions and using the results as guidelines for the higher sucrose concentrations. In this procedure we found that k_f and k_r varied in tandem, in accord with the fact that the pK (of the ground state) was independent of the sucrose concentration. Thus, as the concentrations of the sucrose increased, we varied k_r in proportion to k_f . The radius of the reaction sphere, R_0 , was initially set as that of pure water. Through the set of sucrose concentration it remained practically constant (within ± 0.25 Å) with no systematic trend. The diffu-

sion coefficient, which we expected to vary sharply with the addition of sucrose, was also constant. In all simulations the iteration procedure led its value to be that of pure water:

$$D_{\text{H}^+} = 9.3 \pm 0.2 \cdot 10^{-5} \text{ cm}^2/\text{s}.$$

Thus, the whole fit of the curves over wide sucrose concentration, from 0 to 2 M, was achieved by only two parameters which did vary, the dielectric constant of the diffusion medium and k_f (and k_r) which quantitate the dynamics at the surface of the reaction sphere.

The dielectric constant of the solution is a continuum property of the diffusion space. The calculated values of ϵ , derived from kinetic measurements carried out at varying sucrose concentrations, are shown in Fig. 2. The line in this figure corresponds with the values published in the International Critical Tables (Hartshorn et al., 1933). The coherence of the two data sets legitimizes the dynamic analysis as a method suitable for quantifying the physical properties of the diffusion space.

The last parameter to be considered is the rate of the reaction on the surface of the reaction sphere. As seen in Fig. 3, both the forward and backward reactions decreased in tandem, following the concentration of sucrose.

Considering the fact that R_0 is invariable, we assign the decrement of the two rates, which proceed on the surface of the reaction sphere, as a term (σ) expressing to what extent sucrose molecules eclipse the perimeter of the reaction sphere.

Diffusion controlled reactions in sucrose solutions

The diffusion controlled reaction between proton and the ground state pyranine anion (Gutman, 1986) was monitored as a transient absorbance at the wavelength of ΦO^- .

In pure water, the reprotonation is fast, completed in 5–10 μs (Fig. 4 *A*). At increasing sucrose concentrations the relaxation is appreciably slower (*B* and *C*, respectively).

The reprotonation of ΦO^- is a homogeneous diffusion controlled reaction described by a nonlinear differential equation (Gutman, 1986).

$$\frac{d\phi\text{O}^-}{dt} = -k_1[[\bar{H}^+ + \bar{\Phi\text{O}^-}]X - X^2] - k_2. \quad (2)$$

In this equation, X stands for the incremental concentration of ΦOH dissociated by the laser pulse, while \bar{H}^+ and $\bar{\Phi\text{O}^-}$ are the equilibrium concentrations of these species. The diffusion controlled rate constant of protonation is given by k_1 , while k_2 is the thermodynamic controlled rate constant of ΦOH dissociation. The pK of the pyranine (ground state) was determined by titrations

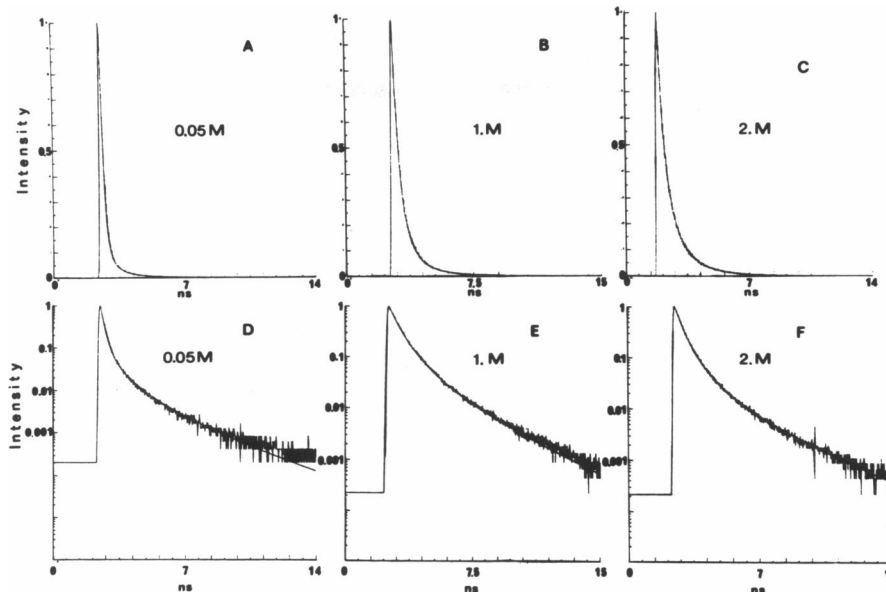


FIGURE 1 Time resolved fluorescence dynamics of pyranine emission. The measurements were carried out with $50 \mu\text{M}$ pyranine in 50 mM, 1 M and 2 M sucrose solution at pH 5.75.

A, B, and C depict the dynamics on a linear *Y* scale; in *D, E, and F* the results are drawn on a logarithmic scale. The smooth curve appearing in each frame is the theoretically reconstructed dynamics.

and found to be constant over the whole range of sucrose concentrations (7.7 ± 0.05), thus, the ratio k_1/k_2 is constant and the dynamics is controlled by a single parameter, k_1 .

To reproduce the slower recombination in sucrose solution we simulated the experimental curves by integration of Eq. 2 using the experimental values of \bar{H}^+ , ΦO^- and X (measured as the amplitude at $t = 0$) with k_1 as adjustable parameter. The dependence of k_1 on the concentration of the sucrose is seen in Fig. 5.

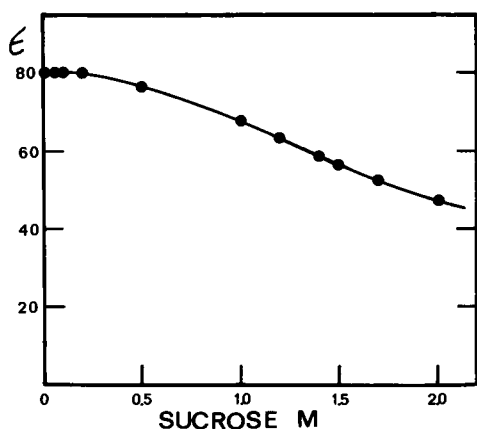


FIGURE 2 The dependence of the dielectric constant of sucrose solution on the molar concentration of the sucrose. The data points appearing on the graph were derived by the numeric reconstruction of fluorescence decay dynamics as exemplified in Fig. 1. The line appearing in the graph was drawn through the data points listed by Hartshorn et al. (1933). (Their data points were omitted for the sake of clarity).

The analysis of the magnitude of k_1 was carried out through the Debye Smoluchowski equation:

$$k_1 = \left(4\pi \frac{N}{1000} \cdot \Sigma D \cdot R_o \cdot \sigma \right) \cdot \frac{\delta}{e^\delta - 1} \cdot e^{\delta R_o \kappa / (1 + R_o \kappa)}. \quad (3)$$

The first group of terms in Eq. 3 denotes the rate of encounter (k_{en}) between two uncharged reactants which form a product when approaching to a distance of R_o . ΣD is the sum of their diffusion coefficient and their fruitful collision has a certain steric restriction $\sigma \leq 1$ (Eigen and Kustin, 1960). The second term in Eq. 2 introduces the long-range electrostatic interactions be-

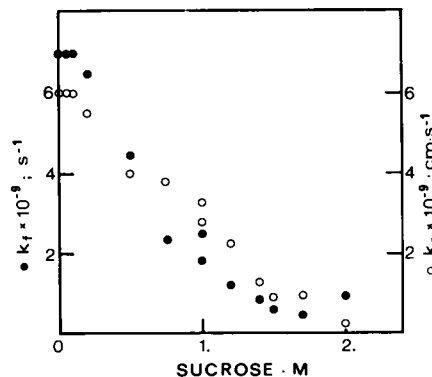


FIGURE 3 The effect of sucrose concentration on the rate of the reactions on the surface of the reaction sphere.

The data points are those derived from the theoretical reconstruction of the dynamics: \bullet k_f is the rate of proton appearance, \circ k_r , the rate of proton absorption.

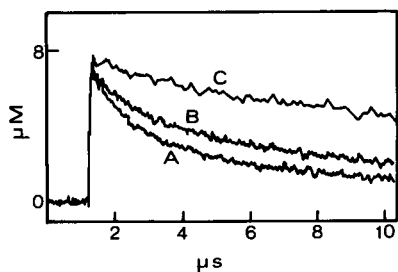


FIGURE 4 The effect of sucrose on the dynamics of reprotonation of ground state pyranine anion. The 50- μ M dye was dissolved in 65 mmol KCl pH 6.7 (A) or supplemented with 0.8 M or 1.9 M sucrose (B and C, respectively). The recording initiates with the excitation pulse of the dye and follows the absorption of the ground state anion at 457 nm. Each curve is an average of 512 pulses.

tween the reactants. Where δ is the ratio between the Debye radius and the radius of contact

$$\delta = Z_1 Z_2 e^2 / \epsilon \cdot kTR_0.$$

As the dielectric constant of the solution decreases, δ will increase, leading to extended long range interactions. The last term in Eq. 3 denotes the Debye Huckel electrostatic screening by the electrolyte with κ as the Debye length.

The experiments were carried out under controlled conditions, allowing to extract from the measured value,

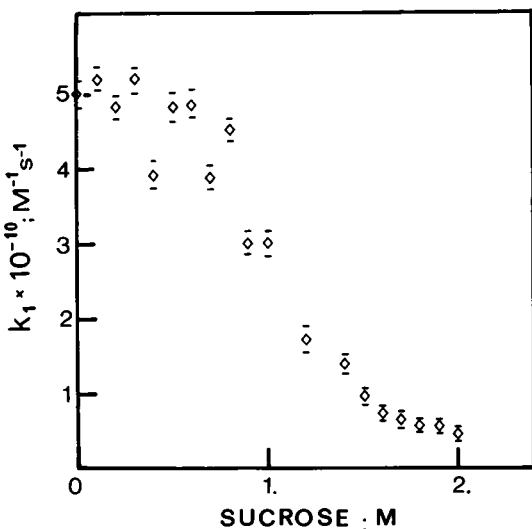


FIGURE 5 The dependence of the second-order rate constant of proton-pyranine anion reaction on the concentration of sucrose. The experiments were carried out as demonstrated in Fig. 4 and analyzed as described in the text to determine the rate constant of the reaction. The 50- μ M dye was dissolved in the indicated sucrose concentration supplemented with KCl at varying concentrations so that the expanded Coulomb cage (due to lower dielectric constant) and increased ionic screening will keep the electrostatic term of the Debye Smoluchowski equation invariable as the sucrose concentration is increased (see Eq. 3).

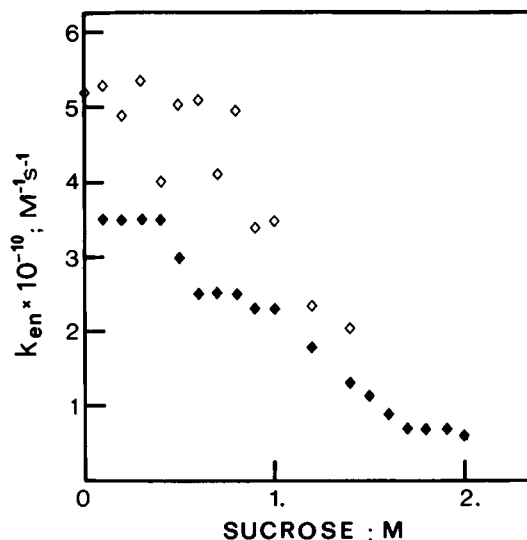


FIGURE 6 The effect of sucrose on the rate of encounter between proton and ground state pyranine anion.

The reactions, measured as in Fig. 4, were analyzed according to Eq. 3 to determine the rate of encounter between the reactants. \diamond Measurements carried out 65 mmol KCl; \blacklozenge measurements carried out in varying concentrations of KCl to keep the contribution of enhanced electrostatic attraction and ionic screening at a constant value equal to 0.82.

the molecular parameter k_{en} . This parameter, shown in Fig. 6, varies with the concentration of sucrose.

Electric conductivity of protons in concentrated sucrose solution

The limiting conductivities of HCl and KCl were measured in varying sucrose concentrations. The results are shown in Fig. 7. The limiting conductivities of the two electrolytes decrease at high sucrose concentrations, yet that of HCl is persistently higher than that of KCl, indicating that the advantage of the Grotthus mechanism for proton propagation over the self-diffusion of K^+ ion, is not abolished.

DISCUSSION

The concentrated solution of sucrose in water is a microscopic dispersion of water in the volume of the solution, a dispersion which hardly affects the chemical potential of the water (Robinson and Stokes, 1959).

That property allowed us to verify to what extent the proton-anion recombination is suitable for quantitating the properties of the medium where the reaction proceeds. As demonstrated in Fig. 2, the dielectric constant deduced from the kinetic analysis is exactly as determined by classical methods.

The diffusion coefficient of proton in sucrose solutions (0–2M) is equal to that in pure water, a finding

based on the subnanosecond dynamics and their numerical reconstruction. The sucrose solution can be regarded as made of small aqueous spaces interspaced between the sucrose molecules, where the connectivity between these spaces is maintained as sucrose molecules execute their Brownian motion. This random connectivity provides a mode by which a proton diffuses from one space to another. The fact that the overall diffusion coefficient is not different from that in bulk water implies that the passage of proton through a temporary connection between two spaces is as fast as in the bulk. As both the diffusion of proton and relative motion of sucrose molecules are random Brownian events, the whole process does not lose its random nature.

Acceptance of these conclusions, derived from the subnanosecond measurements, is instrumental for understanding the microsecond dynamics. When interpreting the dependence of k_{en} on the sucrose content of the solution (Fig. 5) according to Eq. 3, one cannot discriminate whether k_{en} decreases due to smaller diffusion coefficient or to a masking of the reaction sphere by the proton impermeable sucrose molecules. As the diffusion coefficient is constant, the effect must be attributed to the steric mechanism.

Agmon's mathematical treatment, based on the time dependent Debye Smoluchowski operator, regards the reaction sphere as a space where the proton transfer dynamics is too fast to be resolved. Similarly, the time independent Debye Smoluchowski equation (Eq. 3) treats the Coulomb cage (where the electrostatic potential is larger than kT) as a volume where the rate of reactions is too fast to be resolved. Thus, R_0 in the formalism of

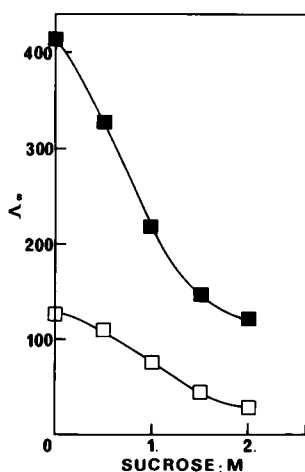


FIGURE 7 The dependence of limited conductivities of HCl (■) and KCl (□) solutions on sucrose solutions.

The conductivities were measured (25°C) at varying electrolyte concentrations 0.5–10 mM. The conductivity of the sucrose solution, without the electrolyte, was subtracted and the values were extrapolated to zero electrolyte concentration. All measurements were carried out in triplicates.

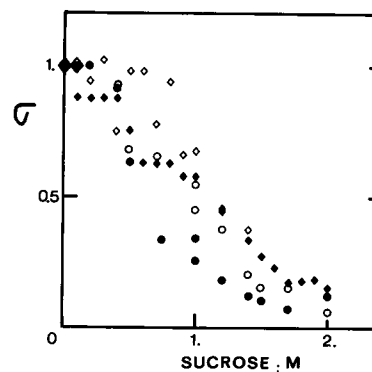


FIGURE 8 The masking of pyranine anion from proton by sucrose. The ordinate denotes the steric factor (σ) defined as the ratio of the rate constant measured at a given sucrose concentration to that measured in pure water. The results depict data gathered at the picosecond time scale (● - k_r and ○ - k_r) and the microsecond time scale (◇ - k_{en} measured at constant KCl concentration, 65 mM; ◆ k_{en} measured with varying KCl concentrations, see legend to Fig. 6).

Agmon, like the radius of the Coulomb cage, is actually the observer's horizon. It is as close as he can see and resolve the reaction by his means.

In Fig. 8, we drew the reactivity on the observer's horizon at a given sucrose concentration normalized to the rate in water. The rate of proton capture and release, in the picosecond and microsecond dynamics, all follow the same function, which we interpret as the partial coverage of the horizon by the proton impermeable sucrose molecules.

This research is supported by the United States-Israel Binational Science Foundation grant 870035 and the US Navy, Office of Naval Research grant N00014-89-J1662.

Received for publication 10 September 1991 and in final form 3 March 1992.

REFERENCES

- Adam, G., and M. Delbruck. 1968. Reduction of dimensionality in biological diffusion processes. *In Structural Chemistry and Molecular Biology*. A. Rice, and N. Davidson, editors, W. H. Freeman and Co., San Francisco, CA. 198–215.
- Agmon, N., and A. Szabo. 1990. Theory of reversible diffusion influenced reactions. *J. Chem. Phys.* 91:5270–5284.
- Agmon, N., E. Pines, and D. Huppert. 1988. Geminate recombination in proton-transfer reactions. II. Comparison of diffusional and kinetic schemes. *J. Chem. Phys.* 88:5631–5638.
- Berg, H. C., and E. M. Purcell. 1977. Physics of chemoreception. *Biophys. J.* 20:193–219.
- Eigen, M., and K. Kustin. 1969. The influence of steric in fast protolytic reactions as studied with HF, H₂S and substituted phenols. *J. Am. Chem. Soc.* 82:5952–5953.
- Gutman, M. 1984. The pH jump: probing of macromolecules and

-
- solutions by a laser-induced, ultrashort proton pulse. Theory and applications in biochemistry. *Methods Biochem. Anal.* 30:1-103.
- Gutman, M. 1986. Application of the laser-induced proton pulse for measuring the protonation rate constants of specific sites on proteins and membranes. *Methods Enzymol.* 127:522-538.
- Gutman, M., and E. Nachliel. 1990. The dynamic aspects of proton transfer processes. *Biochem. Biophys. Acta.* 1015:391-414.
- Hardt, S. L. 1979. Rates of diffusion controlled reactions in one, two and three dimensions. *Biophys. Chem.* 10:239-243.
- Hartshorn, L., C. C. Harris, J. A. Hay, T. I. Jones, and A. G. Milligan. 1933. Dielectric constants and dielectric strength of single crystals, mixtures and solutions, pure organic solvents and miscellaneous materials. International Critical Tables VI, McGraw Hill, Inc., New York. 82-106.
- Huppert, D., E. Pines, and N. Agmon. 1990. The long time behavior of reversible geminate recombination. *J. Opt. Soc. Am.* 7:1545-1550.
- Kjellander, R., and S. Marcelja. 1988. Inhomogeneous Coulomb fluids with image interactions between planar surfaces. III. Distribution functions. *J. Chem. Phys.* 88:7138-7146.
- Mathias, R. T., G. J. Baldo, K. Manivannan, and S. McLaughlin. 1991. Discrete charges on biological membranes. In *Electrified Interfaces in Physics, Chemistry and Biology*. R. Guidelli, editor. Kluwer Academic Publishers Dordrecht, Holland. In press.
- Matthew, J. B., and F. M. Richards, 1982. Anion binding and pH-dependent electrostatic effects in ribonuclease. *Biochemistry.* 21:4989-4999.
- Pines, E., D. Huppert, and N. Agmon. 1988. Geminate recombination in excited-state proton transfer reactions: Numerical solution of the Debye-Smoluchowski equation with back reaction and comparison with experimental results. *J. Chem. Phys.* 88:5620-5630.
- Robinson, R. A., and R. H. Stokes, 1959. In *Electrolyte Solutions*. Butterworth Scientific Publications, London.